

Optical pulse shaping using optical coherent transients

Zeb W. Barber, Mingzhen Tian, Randy R. Reibel, and W. Randall Babbitt

Montana State University, Dept. of Physics, Rm 264 EPS Bldg., Bozeman, MT 59717-3840

zwb@montana.edu

Abstract: Using multiple temporally-overlapped, frequency offset and phase-tuned, linear frequency chirps, a new method of multi-GHz optical coherent transient optical pulse shaping and processing in inhomogeneously broadened rare-earth doped crystals is proposed. Using this technique with properly chirped laser sources, multi-GHz processing can be controlled with conventional low-bandwidth electronics and optical modulators. Specifically, this technique enables pulse shaping in the MHz to THz frequency regime with time-bandwidth-products exceeding 100,000, filling the gap between the operating regimes of femtosecond pulse shaping and analog electronics. The low bandwidth (~20 MHz) proof-of-concept demonstrations presented in this paper include pulse train creation, self-convolution, auto-correlation, and chirped pulse compression.

©2002 Optical Society of America

OCIS codes: (300.6240) Spectroscopy, coherent transient; (320.5540) Pulse shaping;

References and Links

1. A.M. Weiner, "Femtosecond optical pulse shaping and processing," *Prog. Quant. Electr.* **19**, 161 (1995).
2. H. Kawashima, M.M. Wefers, and K.A. Nelson, "Single-pulse and multiple-pulse femtosecond spectroscopy: progress toward collective mode-selective chemistry," *Physica B* **219&220**, 734 (1996).
3. X. Ribeyre, C. Rouyer, F. Rauolt, D. Husson, C. Sauteret, and A. Migus, "All-optical programmable shaping of narrow-band nanosecond pulse with picosecond accuracy by use of adapted chirps and quadratics nonlinearities," *Opt. Lett.* **26**, 1173 (2001).
4. H. Schwoerer, D. Erni, and A. Rebane, "Holography in frequency selective media III. Spectral synthesis of arbitrary time-domain pulse shapes," *J. Opt. Soc. Am. B* **12**, 1083 (1995).
5. H. Sónajalg, A. Gorokhovskii, R. Kaarli, V. Palm, M.Rätsep and P. Saari, "Optical Pulse Shaping by Filters Based on Spectral Hole Burning," *Opt. Commun.* **71**, 377 (1989)
6. S. Altner, S. Bernet, A. Renn, E. Maniloff, F. Graf, U.P. Wild, "Spectral holeburning and holography VI: Photon echoes form cw spectrally programmed holograms in a Pr³⁺:Y₂SiO₅ crystal" *Opt. Commun.* **120**, 103 (1995)
7. G.C. Bjorklund, "Optical pulse shaping device and method," U.S. Patent 4 306 771 (1981).
8. R. L. Cone, R. W. Equall, Y. Sun, R.M. Macfarlane, and R. Hutcheson, "Ultraslow dephasing and dephasing mechanisms in rare earth materials for optical data storage," *Laser-Phys.* **5**, 573 (1995).
9. R. Reibel, Z. Barber, M. Tian, W.R. Babbitt, "Temporally overlapped linear frequency-chirped pulse programming for true-time-delay applications," *Opt. Lett.* **27**, 494 (2002).
10. R. Reibel, Z. Barber, M. Tian, W.R. Babbitt, "High Bandwidth Spectral Gratings Programmed with Linear Frequency Chirps," *J. of Lumin.* **98**, 355 (2002)
11. L. Ménager, L. Caberet, I. Lorgeté, and J.-L. Le Gouët, "Diode Laser extended cavity for broad-range fast ramping," *Opt. Lett.* **25**, 1246 (2000).
12. L. Levin, "Mode-hop-free electro-optically tuned diode laser," *Opt. Lett.* **27**, 237 (2002).
13. X. Wang, M. Afzelius, N. Ohlsson, U. Gustafsson, S. Kröll, "Coherent transient data-rate conversion and data transformation," *Opt. Lett.* **25**, 945 (2000).
14. Y.S. Bai and T.W. Mossberg, "Experimental studies of photon-echo pulse compression," *Opt. Lett.* **11**, 30 (1986)
15. L. Ménager, I. Lorgeté, J.-L. Le Gouët, R. Mohan Krishna, and S. Kröll, "Time-domain Fresnel-to-Fraunhofer diffraction with photon echoes," *Opt. Lett.* **24**, 927 (1999)
16. R. Reibel, Z. Barber, M. Tian, W.R. Babbitt, Z. Cole, K.D. Merkel, "Amplification of High Bandwidth Phase Modulated signals at 793nm," *J. Opt. Soc. Am. B* **19**, 2315 (2002)
17. K.D. Merkel and W.R. Babbitt, "Compensation for homogeneous dephasing in coherent transient optical memories and processors," *Opt. Commun.* **128**, 136 (1996)

1. Introduction

Optical pulse shaping is the creation of a complex optical waveform from a single pulse, especially when one cannot create the complex waveform directly. Pulse shaping of femtosecond pulses has been extensively studied [1], and utilized in applications such as coherent control of simple molecular processes [2]. Other applications have been proposed, including production of dark solitons for long haul fibers, optical time domain multiplexing, optical code-division multiple access multiplexing, and chirped pulse compression. Most methods of optical pulse shaping in the femtosecond to picosecond regime involve gratings to spatially disperse the frequency components of a pulse, which is then modulated using spatial light amplitude and phase modulators. Due to the limited resolution of gratings and spatial light modulators these techniques have frequency resolution of ~ 10 GHz making 100ps the maximum temporal duration of the pulse packet. Other methods of pulse shaping utilize beamsplitters and physical delay lines or chirped pulses and dispersive elements to create a desired temporal shape [1, 3, 4]. Previous pulse shaping techniques utilizing the photon echo process modulated slowly scanned laser beams to sculpt frequency dependent gratings in a holeburning medium that then shaped incoming optical waveforms [5-7]. The required frequency, amplitude, and phase control of the laser beams limited the performance of these approaches. None of the above methods allowed for a practical, rapidly programmable means of achieving high time-bandwidth product pulse shaping up to the nanosecond regime.

In this paper, we propose and experimentally demonstrate a method to perform pulse shaping using optical coherent transient (OCT) processes in inhomogeneously broadened holeburning medium, such as cryogenic rare-earth ion doped crystals. These crystals can have inhomogeneous linewidths up to 100 GHz, homogeneous linewidths as narrow as 1 kHz, and allow time-bandwidth products of 10^4 - 10^6 [8]. Methods similar to [4] could be utilized, but would rely on pulsed lasers and long delay lines. The technique we propose utilizes the broad bandwidth available from chirped laser pulses, but requires only low bandwidth (MHz) electronics and modulators to control the multi-GHz output waveform. Our technique differs from the technique described in [5-7] where the frequency grating is incoherently written. Our technique writes the grating coherently; allowing better phase control, better temporal resolution, faster programming times, and more flexibility in the choice of probe pulses.

2. Theory

In previous papers, we demonstrated that two temporally overlapped linear frequency-chirped pulses (TOLFCs) could be utilized to create periodic (true time delay) spectral gratings in rare-earth ion doped crystals [9,10]. A brief probe pulse incident upon this grating produces a brief echo output with a delay $\tau_d = \delta/\alpha$. Here δ is the frequency offset between the two chirps and α is their common chirp rate. The TOLFC method has many advantages over brief pulse and temporally separated linear frequency chirped pulse programming, including chirp durations longer than the coherence time of the rare-earth ions (lowering laser power requirements), the ability to use a single chirp source for the programming pulses (reducing laser stability problems), and large delay tuning range ($\sim \mu$ s) using small frequency offsets (\sim MHz). With the development of high bandwidth (>40 GHz) chirped lasers [11,12], the TOLFC method offers an attractive approach to high bandwidth OCT processing.

Using multiple frequency-offset TOLFCs, one can create several time delay gratings, instead of one. Fig. 1 diagrams the multiple TOLFC programming method for use as a pulse shaper. A reference linear frequency chirp, $C_1(t)$, and control chirps, $C_2(t)$, with the desired frequency offsets are temporally and spatially overlapped in the inhomogeneous broadened material to create a complex spectral grating. Later the pulse to be shaped, $E_3(t)$, is diffracted off the grating producing multiple echoes. In general, the desired output signal of a pulse shaper can be written in a generalized form as

$$E_s(t) = \sum_{n=1}^N A_n b_a(t - n\tau) \quad (1)$$

Here τ is the desired sampling period, A_n are complex amplitudes, and b_a is a temporally brief pulse with bandwidth, B_a . In the linear excitation regime, the output echo field of the stimulated photon echo process has a Fourier transform $E_s(\omega) \propto E_1^*(\omega)E_2(\omega)E_3(\omega)$, where $E_i(\omega)$ ($i = 1, 2$ and 3) are the transforms of the reference, the control, and the probe fields, respectively. By choosing the reference and the control pulses properly, a probe pulse can be shaped into an output pulse of arbitrary shape. If the pulse to be shaped is brief, $E_3 = b_a(t)$, the action needed to create the desired output signal, $E_s(t)$, is equivalent to the creation of multiple delayed copies of the input pulse with the proper complex amplitudes. Assume that the reference pulse is a linear frequency chirp, $C_1(t) \propto \exp(i\omega_1 t + i\frac{1}{2}\alpha t^2)$ with bandwidth, $B \geq B_a$, with a chirp rate, α , and a start frequency ω_1 . The required control pulse then has the form, $E_2 \propto \sum_n A_n C_1(t - n\tau)$, which is a linear superposition of delayed copies of the reference chirp, each weighted by A_n . The control pulse can be rewritten as

$$E_2(t) \propto C_1(t) \sum_{n=1}^N A_n \exp(-i\alpha n\tau t - i\omega_1 n\tau + i\frac{1}{2}\alpha(n\tau)^2) \quad (2)$$

If the delays are much shorter than the chirp duration, the delays ($n\tau$) can be replaced with angular frequency shifts of $n\delta = \alpha(n\tau)$ and the required control pulse becomes

$$E_2(t) \propto C_1(t) \sum_{n=1}^N A_n \exp\left(-in\delta t - i\omega_1 n \frac{\delta}{\alpha} + i \frac{(n\delta)^2}{\alpha}\right) \quad (3)$$

This produces multiple TOLFCs with different frequency offsets weighted by the complex amplitudes A_n . If a is small, the frequency shift needed to produce the delay is also small, allowing low bandwidth control of broadband chirps by increasing the chirped pulse time. The additional phase term, $\phi_n = \frac{1}{\alpha}(-\omega_1 n\delta + (n\delta)^2)$, ensures the echo has the same phase regardless of delay, with relative phase between echoes controlled by the A_n 's.

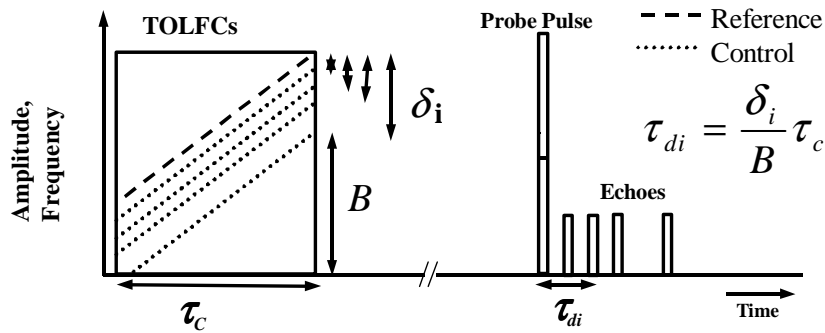


Fig. 1. The TOLFC pulse shaping process. Multiple linear frequency chirps with different starting frequencies (dotted lines) are temporally overlapped with a single higher frequency reference chirp (dashed line). Later a brief probe pulse is diffracted off the grating producing multiple echoes. In the real programming process, the maximum frequency offset is much less than the bandwidth of the chirps.

The proposed pulse shaping method is not limited to brief probe pulses. To shape an arbitrary probe pulse into a new arbitrary output shape with a given bandwidth and sampling rate, one only needs to work out the right set of the complex weighting factors, A_n , needed on

the control pulse. For example, to turn the pulse train, $E_3(t) = \sum_{n=1}^N A_n b_a(t - n\tau)$, into its self-convolution, one can use the reference chirp and control pulses as discussed above. To produce the auto-correlation one uses the control pulse needed to create the time reverse of $E_3(t)$.

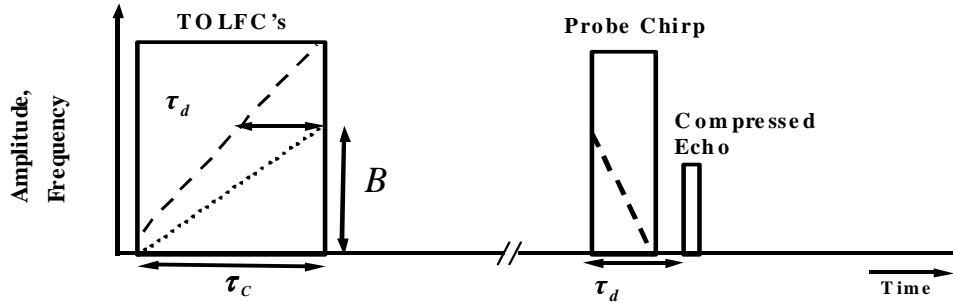


Fig 2. The TOLFC chirp compression process. Two temporally overlapped chirps with different chirp rates and frequency offsets create a linearly-chirped, time-delay grating, which compresses the probe chirp into a delayed transform-limited pulse.

Another application of pulse shaping is chirped pulse compression. Previous studies have shown that OCT's have the ability to compress chirped pulses [13,14]. Here we show that the linear frequency chirps need not be temporally separate and generalize chirp compression to the TOLFC method. A reference chirp and a frequency offset control chirp with different chirp rates α_1 and α_2 , respectively, are used as shown in Fig. 2. One can solve α_2 analytically if $|E_1(\omega)|$ and $|E_2(\omega)|$ are uniform over the bandwidth of the probe pulse (i.e. they are broadband chirps). To compress the chirped probe pulse to its Fourier transform limit, $E_s(t) \propto b_a(t - \tau_d)$, one can set the control chirp as, $E_2(\omega) \propto E_1(\omega)E_3^*(\omega)E_s(\omega)$, where $E_1(\omega)E_3^*(\omega)$ is equivalent to a linear frequency chirp with chirp rate $\alpha_2 = (\alpha_1\alpha_3)/(\alpha_3 - \alpha_1)$. Note this equation is similar to the lens equation, suggesting the formation of a temporal lens in the spectral grating [15]. The control pulse then takes the form of $C_2(t) \propto \exp(i\omega_1(t - \tau_d) + i\frac{1}{2}\alpha_2(t - \tau_d)^2)$, which is a temporally delayed chirp. Here τ_d is the delay time of the echo pulse with respect to the leading edge of the probe pulse and is confined to less than T_2 and greater than the probe chirp duration plus $1/B$. Since the delay is a function of the frequency, τ_d is also the delay of the probe chirp's start frequency. For the case of a limited time bandwidth product, the control chirp takes the same form and the compressed pulse becomes a bandwidth limited brief pulse. For temporally overlapped reference and control chirps, the expression for the delay is now a function of RF frequency ω , frequency offset δ , and chirp rates α_i , given by $\tau_d(\omega) = \frac{\omega}{\alpha_2} - \frac{\omega}{\alpha_1} + \frac{\delta}{\alpha_1}$. Using this method, a multi-GHz chirp of several microseconds in duration can be compressed to its Fourier transform limited duration, roughly the reciprocal of its bandwidth.

3. Experiments

Proof-of-concept demonstrations of the TOLFC pulse shaper for the different processes described above were performed. Acoustic-optic modulators (AOMs) were used to create the linear frequency chirps, limiting these initial demonstrations to 20 MHz. Experiments were performed using an external cavity diode laser with an injection locked amplifier lasing at the ${}^3\text{H}_4\text{-}{}^3\text{H}_6$ transition in $\text{Tm}^{3+}:\text{YAG}$ (~ 793 nm) [16]. The laser beam was split with a 50/50 beam

splitter, passed through two separate AOMs driven by arbitrary waveform generators to create the reference and control chirps. The two beams were then focused to a waist of $\sim 60 \mu\text{m}$ and overlapped in the crystal. The crystal was cooled to $\sim 4.5 \text{ K}$. Powers before the crystal were $\sim 15 \text{ mW}$ on each path. The echo output was incident onto a 50 MHz amplified silicon photodetector. The RF waveform used to program the reference chirp was $\sin(2\pi f_1 t + \frac{1}{2}\alpha t^2)$, where f_1 is the start frequency of the chirp. The control chirps were frequency offset copies of the reference chirp given in Eq (3).

First we tested the pulse shaper's ability to produce pulse trains with arbitrary times and phases. The goal was to program two complex spectral gratings that produced the 11 bit Barker code (11100010010) in both amplitude (AM) and phase modulated (PM) forms at 10 Mbits/sec . Programming chirps were $5 \mu\text{s}$ long with 20 MHz bandwidth giving a chirp rate of $4 \text{ MHz}/\mu\text{s}$. The frequency offset between individual control chirps needed to produce the 10 MHz bit rate was 400 kHz . The bits were controlled via the phase and amplitude of each control chirp. For "1" bits, $A_n = 1$. For "0" bits, $A_n = 0$ for AM and $A_n = -1$ for PM. A 100 ns probe pulse processed by the two different complex gratings produced the expected code in both the binary AM coding (Fig. 3a) and the bi-phase $(0, \pi)$ PM coding (Fig. 3b). The phase encoding $(0, \pi)$ is observed as nulls at phase transitions in Fig. 3b. The exponential homogeneous decay of the output was compensated for by adjusting the relative amplitude of each control chirp, A_n , creating uniform bit amplitudes across the echoed data sequence [17].

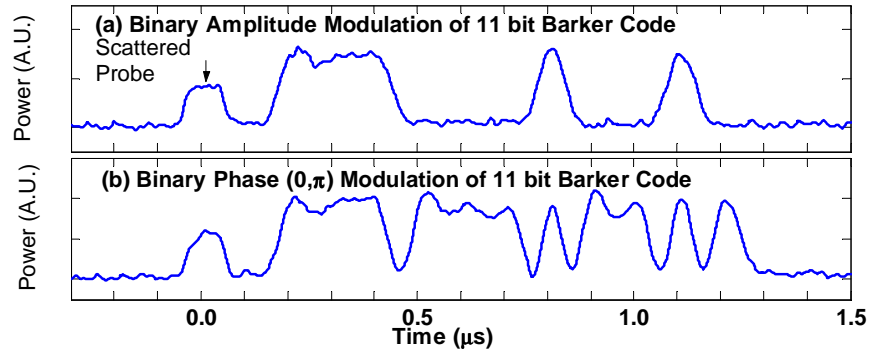


Fig. 3 The echo output of the pulse shaper probed with a 100 ns brief pulse. Output is the binary representation of the 11 bit Barker code (11100010010) in (a) binary amplitude modulated $(0,1)$ format and (b) a binary phase modulated $(0, \pi)$ format.

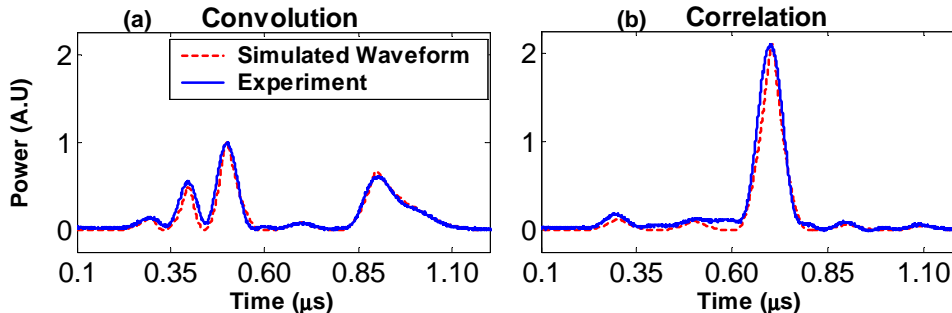


Fig. 4. The calculated (dashed curve) and experimental (solid curve) output of the pulse shaper programmed with the (a) time reverse of the bi-phase 5 bit Barker code $(1,-1,1,1,1)$ and (b) the time forward $(1,1,1,-1,1)$. The operations of (a) self-convolution and (b) auto-correlation were performed on the probe pulse $(1,-1,1,1,1)$.

The ability of the pulse shaper to reshape arbitrary probe pulses was tested next. We demonstrated this by programming the bi-phase 5-bit Barker code $(1,1,1,-1,1)$ and the time-reverse $(1,-1,1,1,1)$ versions of the code into the material. We then probed each grating with

(1,-1,1,1,1). This yielded the operations of self-convolution and auto-correlation of the probe pulse, respectively. This also tested the pulse shaper's phase control. In the first experiment since only the intensity of the output waveform was detected, phase transitions appeared only as nulls in the output. For faithful correlation and convolution, the phase must be well controlled. The theoretical outputs (with decay) are shown in Fig. 4 along with the experimental outputs of the pulse shaper. The agreement between the experiment and calculated outputs confirms that good phase control is obtained.

Finally we used this TOLFC pulse shaping method to perform linear frequency chirped pulse compression of a 1 μs chirped pulse with a $-20\text{ MHz}/\mu\text{s}$ chirp rate. For a 6 μs long 20 MHz up chirped reference pulse, the required chirp rate for the second chirp is 4 MHz/ μs . An offset of 0.3 MHz was added to the second chirped pulse giving a $\sim 90\text{ ns}$ delay between the end of the chirped probe and the echo. Fig. 5 shows the probe chirp and the compressed echo output. The temporal width of the echo measured at $1/4$ the intensity was 64 ns. This gives a compression factor of ~ 16 with compressed echo duration close to the expected of 50 ns for a 20 MHz bandwidth limited pulse. As the chirped bandwidth of the pulses increases, the compression factor should increase. This ability to compress chirps can be combined with the basic multiple-TOLFC process described above. By adding more control chirps to create multiple chirp-compressing gratings with different time delays and choosing the proper delays and phases of these compressed echoes, a multi-GHz chirped probe pulse can produce a multi-GHz analog optical signal with arbitrary shape of nanosecond to microsecond duration.

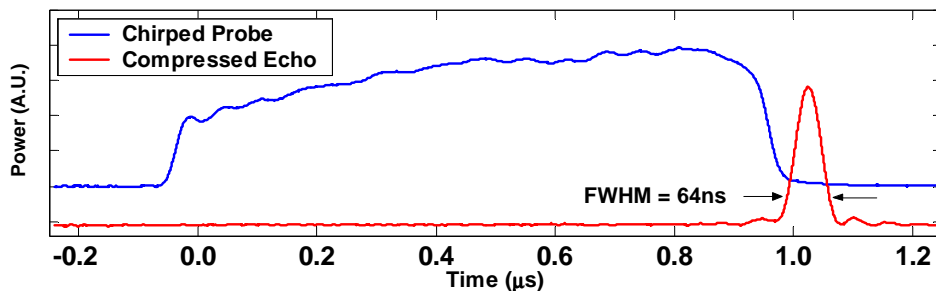


Fig. 5. Test of chirped pulse compression. A 1 μs , 20 MHz chirp (light curve) was diffracted off a chirp compressing grating producing the narrow echo (dark curve). The full width half max of the echo measured at one quarter the intensity is 64 ns, close to the bandwidth limit. The probe and echo are plotted on different scales.

4. Conclusion

We have demonstrated the ability to perform pulse shaping in rare-earth ion doped cryogenic crystals using multiple, temporally overlapped linear frequency chirps. In addition to being able to shape brief pulses into arbitrary waveforms, this versatile OCT pulse shaper can perform pulse shaping on arbitrarily shaped probe signals, including chirps, as well as perform the operations of convolution, correlation, and compression. Unlike previous demonstrations of OCTs, such as true time delay and optical memory, where the output echo mimicked one of the three input pulses, this new programming method produces a unique and well-controlled output signal of arbitrary shape. Recently developed high bandwidth chirped external cavity diode lasers make it possible to control the shape of multi-GHz output signals with only low bandwidth (MHz) electronics and acoustic-optic modulators.

Acknowledgements

We gratefully acknowledge the U.S. Air Force Office of Scientific Research for their support under grant number F49620-98-1-0283. We thank Krishna Rupavatharum and Kris Merkel of the MSU Spectrum Lab for useful discussions on arbitrary waveform generation.